The Fe3+:Sapphire Whispering Gallery Modes Maser Oscillator

P.-Y. Bourgeois, K. Benmessai, M. Oxborrow, M. E. Tobar, Nadine Bazin, J. G. Hartnett, Y. Kersalé, V. Giordano

▶ **To cite this version:**

P.-Y. Bourgeois, K. Benmessai, M. Oxborrow, M. E. Tobar, Nadine Bazin, et al.. The Fe3+:Sapphire Whispering Gallery Modes Maser Oscillator. IEEE International Frequency Control Symposium, May 2007, Genève, Switzerland. 10.1109/FREQ.2007.4319237 . hal-00782279

HAL Id: hal-00782279
https://hal.science/hal-00782279

Submitted on 18 May 2021

HAL is a multi-disciplinary open access archive for the deposit and dissemination of scientific research documents, whether they are published or not. The documents may come from teaching and research institutions in France or abroad, or from public or private research centers.

L'archive ouverte pluridisciplinaire **HAL**, est destinée au dépôt et à la diffusion de documents scientifiques de niveau recherche, publiés ou non, émanant des établissements d'enseignement et de recherche français ou étrangers, des laboratoires publics ou privés.

Distributed under a Creative Commons Attribution 4.0 International License

The Fe^{3+}: Al_2O_3 Whispering Gallery Mode Maser Oscillator

P.-Y. Bourgeois[1], K. Benmessaï[1], M. Oxborrow[2], M. E. Tobar[3], N. Bazin[1], J. G. Hartnett[3], Y. Kersalé[1] and V. Giordano[1]

[1] Institut FEMTO–ST, Dpt. LPMO, UMR 6174 CNRS-Université de Franche-Comté
32 av. de l'Observatoire, 25044 Besançon Cedex, France

[2]National Physical Laboratory
Queens Road, Teddington,Middlesex, TW11 0LW, UK.

[3]The University of Western Australia, FSM group
35 Stirling Hwy, 6009 Crawley, WA, Australia

email : pyb@femto-st.fr

***Abstract*— The Fe^{3+}: Al_2O_3 Whispering Gallery Mode Maser Oscillator is presented in this paper. Preliminary results already show a frequency stability of about 10^{-14} for integration times up to 30 s. A model combining the rate equations and the electromagnetic field in the sapphire is presented. Paramagnetic properties and maser sensitivity to external parameters have been conducted to verify the validity of our model.**

I. Introduction

A number of scientific and technical applications requires very high frequency stability oscillators in the 10^{-14} range. Essential for metrological issues, deep space tracking, radar systems and fundamental physics such as Lorentz invariance violation theories, the Cryogenic Sapphire Resonator Oscillator (CSRO) is generally considered as the unique solution nowadays to reach such performances. An alternative/promising way to the CSRO is the 'WHIGMO' (WHIspering Gallery mode MASER Oscillator). At the end of the year 2004 was discovered, at FEMTO-ST Institute, a bistability effect in a cryogenic Fe^{3+} doped sapphire whispering gallery mode resonator. This effect is similar to that of lasers containing a saturable absorber [9]. Combining then a zero-field 3-level atomic system in the sapphire lattice with the very high Q-factor of the resonator at cryogenic temperatures (Q$\sim 10^9$@ 4 K), the first whispering gallery mode MASER oscillator became possible in the early 2005 at FEMTO-ST [1]. Research about this topic is currently being undertaken through an *ad hoc* international scientific collaboration involving the NPL (National Physical Laboratory) and UWA (the University of Western Australia).

II. The Fe^{3+} MASER Oscillator

Among the different paramagnetic impurities that can be found in high purity sapphire crystal there is the Fe^{3+} ion presenting at zero dc magnetic field three levels: $|1/2\rangle$, $|3/2\rangle$ and $|5/2\rangle$. Near the liquid helium temperature, there are significant differences in the populations of these levels. Transitions between any of these levels are allowed and their linewidths are of a few tens of MHz. A 31.3 GHz pump signal causes a net transfert of Fe^{3+} ions from the $|1/2\rangle$ level to the $|5/2\rangle$ level. In turn non-radiative transitions $|5/2\rangle \mapsto |3/2\rangle$ create a negative population difference between the two lower states, making possible maser oscillation at 12.04 GHz if the resonator presents a high-Q mode at this frequency. The principle of our first whispering-gallery-mode maser oscillator (WhigMO) is represented in Figure 1. It is based on sapphire resonator whose $WGH_{17,0,0}$ mode frequency coincides with the $|1/2\rangle \mapsto |3/2\rangle$ frequency, i.e. 12.04 GHz. Another WG mode at 31.3 GHz is used to pump the cristal. A 2mW pump signal generated by a microwave synthetizer is sufficient to obtain a -56dBm maser signal, available outside of the cryostat.

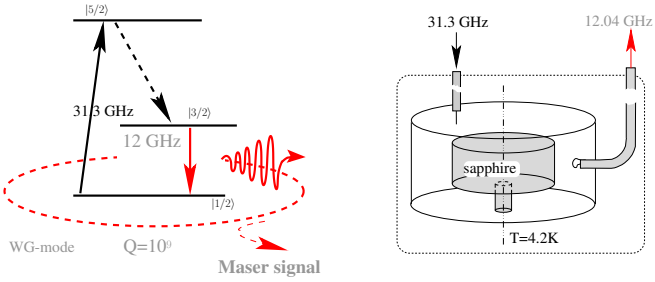

Fig. 1. Principle of the whispering gallery mode maser oscillator.

The validity of the maser operation has been demonstrated at FEMTO-ST in early 2005 with this simple cryogenic experiment. With only a temperature control at the turning point at 8 K, preliminary results shown a 2.5 $\times 10^{-14}$ frequency

instability at 32 seconds by comparing the maser with a microwave synthesizer referenced to a hydrogen maser.

To measure the short term frequency instability it is possible to compare two masers providing a frequency separation of a few hundreds of kHz. The signal resulting from the comparison can then be directly sent to a high resolution low frequency electronic counter. The Allan deviation is finally computed from the extracted frequency data over the integration time. The major problem of this technique is mixing to low-power signals. It could be then an opportunity to compare the maser to a cryogenic sapphire resonator oscillator oscillating on the $\mathrm{WGH}_{17,0,0}$ mode by using the twin resonator of the maser. Nevertheless in our case, we conducted some experiment to compare the maser signal to the state-of-the-art CSRO from UWA and operating at 11.200 GHz. In the case of comparing ultrastable oscillators with operating frequencies differences $>>$100 kHz, the use of an external microwave synthesis chain is required to generate the appropriate beatnote. Figure 2 shows the simplified setup used for the comparison. The beatnote between the CSRO and the maser produces a 838 MHz signal.

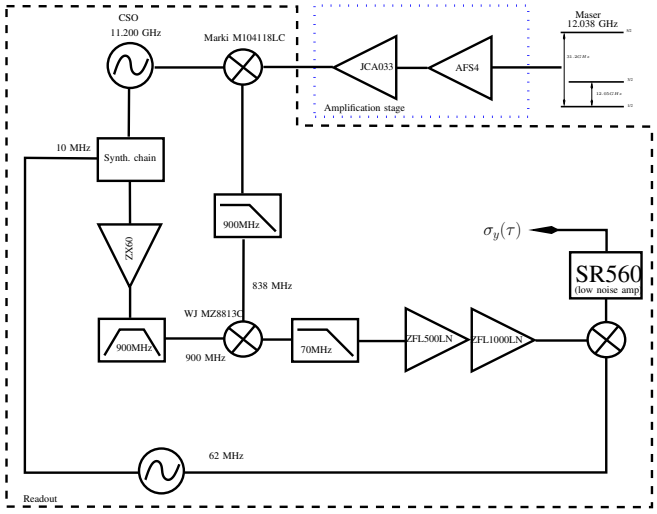

Fig. 2. Frequency stability measurement scheme : maser vs UWA's CSO

Through the microwave synthesis chain, the 9th harmonics of a 100 MHz signal locked to the CSRO and referenced by a hydrogen maser is mixed with the previous signal. The mixing stage delivers a 62 MHz signal. An external 62 MHz low-frequency generator locked to the microwave synthesis chain delivers the required 62 MHz signal used to downconvert the microwave beatnote to some 100 kHz. Finally the obtained signal feeds a low noise preamplifier and is send to a high resolution low-frequency reciprocal counter.

In order to qualify the noise budget of the overall readout system we have used a noise measurement bench as shown on figure 4.

The maser frequency instability is short-term limited by the microwave synthesis chain at 10^{-14} up to 30 s as shown on figure 3. For integration times higher than 30 s, the

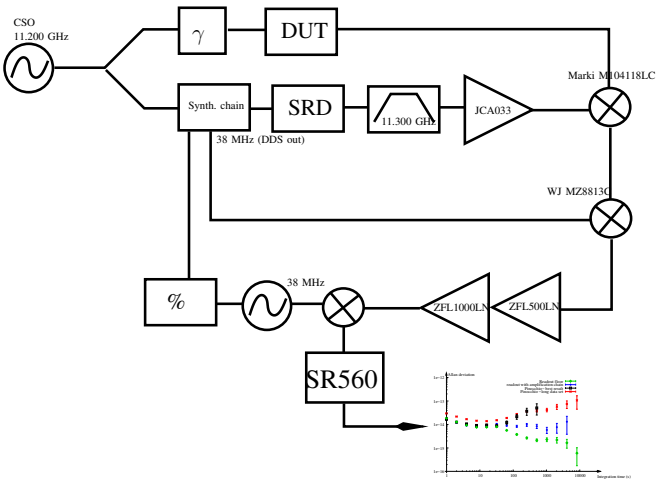

Fig. 3. Bench scheme for the readout system noise measurement.

maser presents a random walk process (characterized by a $\sqrt{\tau}$ slope.). This effect is probably due to the pump power fluctations.

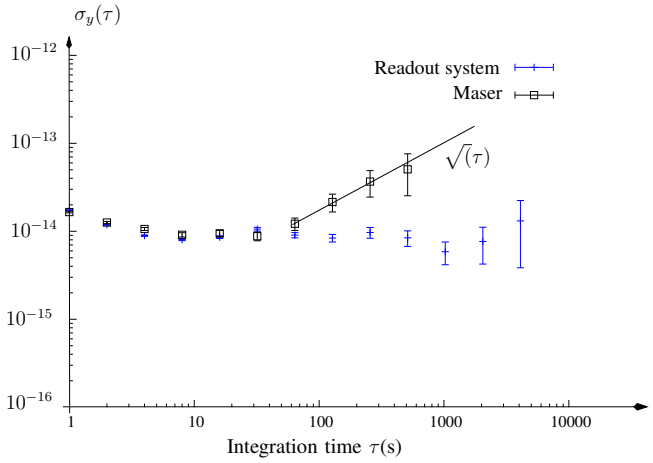

Fig. 4. Allan deviation of the readout system and the maser.

III. The Fe^{3+} : Al_2O_3 resonator bistability

Usually the transmission coefficient of WG modes is independent of the injected power at the resonator input. In our experiment, for a particular mode (*i.e.* $\mathrm{WGH}_{17,0,0}$ at 12.038 GHz) we observed a non linear response for the transmission coefficient versus the injected power, while for others modes (for example the $\mathrm{WGH}_{18,0,0}$ at 12.6 GHz) the response appears totally linear (fig.5).

Compared to the typical behavior of a common WGH-mode, our relevant $\mathrm{WGH}_{17,0,0}$ mode clearly presents two thresholds depending on the direction of the power sweep. It has also been observed that the hysteresis bandwidth is a function of temperature. This bistability phenomenon can only be explained by the saturation of the Fe^{3+} ions at 12.04 GHz, which is analogous to that of "optical bistability" exhibited by

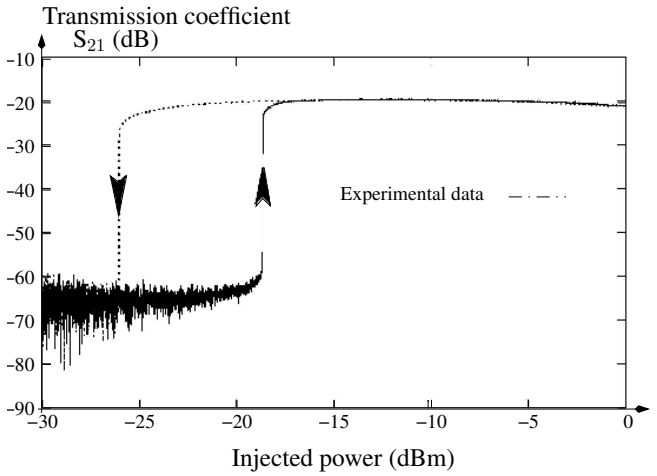

Fig. 5. Anomalous resonator behavior at 12 GHz.

a saturable absorber. Starting from -30 dBm, for low applied powers the $\mathrm{WGH}_{17,0,0}$ mode is embedded into the noise floor: the whole atomic system is purely absorbtive. By increasing slightly the injected power to -18.6 dBm the saturation process starts. This induce stored energy enhancement which in turn enhances the saturation process until the system becomes bistable. At this point, the mode $\mathrm{WGH}_{17,0,0}$ would suddenly appear and its behavior become then similar to other "normal" modes when increasing the injected power. Conversely, starting from a completely saturated Fe^{3+} transition state and decreasing power, the second threshold appears at a lower power (-26 dBm) than in the first case, in the sense that enough energy still remains in the system to deliver the resonance before vanishing into the noise again.

A. Transmission line model for a resonator without impurity

The WGM resonator can be assimiled to a dielectric wave guide out of ring.

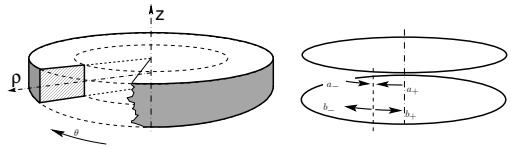

Fig. 6. *Modeling of a whispering gallery mode resonator.*

This dielectric guide constitutes a closed transmission line (figure 6, right). It's impedance Z_c can be calculated by the knowledge of the geometrical and physical properties of the resonator. In this line two waves a_+ and a_- can be propagated in opposite directions. If the resonator is perfect then the two waves are uncoupled. In this condition the resonance imposes that the phase Φ accumulated on a ring turn is equal to $2m\pi$.

$$\begin{cases} a_-(\theta) = a_-(\theta)e^{-j\Phi} \\ a_+(\theta) = a_+(\theta)e^{-j\Phi} \end{cases} \Longrightarrow \Phi = 2m\pi \tag{1}$$

Then the voltage along the ring is:

$$V(\theta) = (a_-(\theta) + a_+(\theta))/\sqrt{Z_C} = V(0)\cos m\theta \tag{2}$$

1) Resonator coupling and unloaded quality factor: The couplings with the external circuit are modelled thanks to hybrid couplers, as indicated on the figure 7.

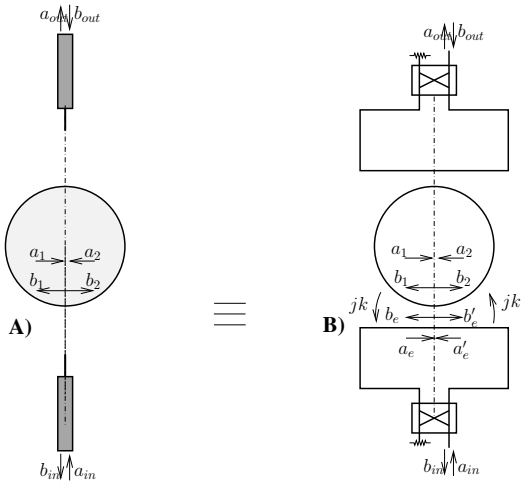

Fig. 7. *Modeling of couplings : A) real resonator coupled by antenna. B) Hybrid couplers modeling.*

In the absence of impurity (or if the paramagnetic transition is satureted), one can show that the resonator unloaded Q factor is :

$$Q_0^{WG} = \omega_0 \frac{\text{Energy stored in the resonator}}{\text{Dissipeted power}} = \omega_0 \frac{W_T}{P_a} = \frac{\mathrm{m}\pi}{\alpha} \tag{3}$$

where α is the wave attenuation coefficient along a turn in the resonator. This term reflects the material dielectric losses tangent (tanδ):

$$\alpha = \mathrm{m}\,\pi\, tan\delta \tag{4}$$

The resonator coupling coefficients β_1 and β_2 are defined as:

$$\beta_1 = \frac{k_1^2}{2\alpha} \quad \text{and} \quad \beta_2 = \frac{k_2^2}{2\alpha} \tag{5}$$

where k_1 and k_2 depends on the geometry of the device coupling.

2) Transmission coefficient S_{21}: The resonator transmission coefficient (S_{21}) can be expressed as [10]:

$$S_{21} = -\frac{k_1 k_2\ e^{-\frac{\alpha + j\Phi}{2}}}{1 - \sqrt{1-k_1^2}\sqrt{1-k_2^2}\ e^{-(\alpha + j\Phi)}} \tag{6}$$

In a WGM resonator, it's justified to consider $k_1,\ k_2,\ \alpha$, and $\Im(\Phi) \ll 1$. In the same way, near the resonance : $\Re(\Phi) \approx 2m\pi$. With these assumptions, S_{21} becomes:

$$S_{21} = -\frac{k_1 k_2}{\frac{k_1^2}{2} + \frac{k_2^2}{2} + \alpha + j(\Phi - 2m\pi)} \tag{7}$$

In the theory of lines Φ can be expressed as a fonction of the wave number, $\Phi = k_g\ R_e$, where R_e is the transmission line equivalent radius.

Then, in the absence of paramagnetic impurities and at a frequency ν, the equation 1 becomes:

$$\Phi = 2\pi k_g R_e = \frac{4\pi^2 R_e \nu}{c}\sqrt{\epsilon_z} \tag{8}$$

with ϵ_z is the sapphire relative permittivity along the resonator C-axis.

B. Two levels system

In order to introduce the important parameters, it is necessary to start with a study of a two levels system. These two levels can correspond to the levels $|1/2>$ and $|3/2>$ of the ion Fe^{3+} ion. In the absence of any pump signal and if the frequency injected into the resonator remains close to 12.04 GHz, the level $|5/2>$ can be temporarily forgotten. Under these conditions the system is equivalent to a spin 1/2. This is for a system with S=1/2 that the following expressions were derived. However, the various expressions which follow can be generalized without much difficulty for a more complex system. The forms of these expressions remain unchanged, only numerical coefficients will vary. Let us consider 2 levels separated by an energy $h\nu_{12}$.

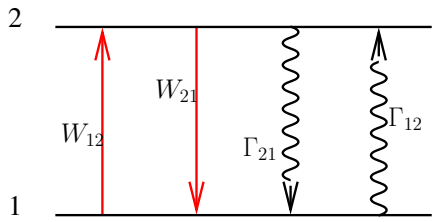

Fig. 8. *Two-level system.*

The dynamics of this ions system subjected to a resonant interaction is described by 4 parameters:
- W_{12}: absorption probability per unit of time. The absorption of an incidental photon induces the transition of the ion from level 1 towards level 2.
- W_{21}: stimulated emission probability per unit of time.
- Γ_{12}: Rate of relaxation $1 \rightarrow 2$. The vibrations of the crystal lattice (phonons) can cause relaxation without absorption of the radiation and thus induce a transition.
- Γ_{21}: Rate of relaxation $2 \rightarrow 1$: idem.

N is the total density of ions, N_1 et N_2 are the populations of the levels at the thermodynamic equilibrium and $\Delta_{12} = \frac{h\nu_{12}}{kT}$:

$$\frac{N_2}{N_1} = e^{-\Delta_{12}} \approx 1 - \Delta \quad \text{for } \frac{h\nu_{12}}{kT} \ll 1 \tag{9}$$

In general, the populations of the two levels are noted n_1 and n_2. The differences of populations will be:

$$\Delta N = N_1 - N_2 \approx \frac{h\nu_{12}}{2kT}N \qquad \text{and} \qquad \Delta n = n_1 - n_2 \tag{10}$$

1) Absorbed power: The absorbed power per volume is equal to (for a spin 5/2):

$$\begin{aligned} dP &= (W_{12}n_1 - W_{21}n_2)\, h\nu dV = W_{12}\Delta n h\nu dV \\ &= \frac{1}{2}\gamma^2 h\nu H^2 \Delta n\ g(\nu)\ dV \end{aligned} \tag{11}$$

where dP and dV are the power and the volume densities respectively, γ the gyromagnetic ratio, H the amplitude of the magnetic field, and $g(\nu)$ the line shape function. A simple form of this function is the *Lorentz line shape*, given by the expression:

$$g(\nu) = \frac{2T_2}{1 + (2\pi T_2)^2 (\nu - \nu_{12})^2} \tag{12}$$

This function has a width $\Delta\nu_{ESR} = \frac{1}{\pi T_2}$ and its value at $\nu = \nu_{12}$ is equal to $2T_2$; two times the *spin-spin* relaxation time.

If the incidental signal is weak, the difference of population is not notably influenced:

$$\Delta n \approx \Delta N \tag{13}$$

The absorbed power will grow proportionally to the intensity of the incidental radiation:

$$dP = \frac{(h\nu_{12})^2 N}{2\pi kT} \frac{(\gamma H)^2}{\Delta\nu_{ESR}}\ dV \tag{14}$$

If the wave intensity is still growing, the difference of population Δn will not remain equal any more to ΔN, the solution of the rate equations gives:

$$\Delta n = \Delta N \frac{1}{1 + 2W_{12}T_1} = \Delta N \frac{1}{1 + 2(\gamma H)^2 T_1 T_2}\delta \tag{15}$$

The thermodynamic equilibrium is broken, and the absorbed power becomes:

$$dP = h\nu_{12}\Delta N \frac{W_{12}}{1 + 2W_{12}T_1}\ dV \tag{16}$$

where $T_1 = (\Gamma_{12} + \Gamma_{21})^{-1}$ is interpreted as the caracteristics time necessary for the system to return to its thermodynamic equilibrium.

At the limit when the power of the signal is very strong, the ions system is saturated and the absorbed power tends towards the limit:

$$\lim_{H\to\infty} dP = \frac{h\nu_{12}\Delta N}{2T_1}\ dV \tag{17}$$

2) Magnetic susceptibility: Macroscopically the presence of the ions in the sapphire matrix is described by the appearance of magnetic susceptibility $\chi(\nu) = \chi'(\nu) + j\chi''(\nu)$. The imaginary part χ" is classically connected to the magnetic losses. Thus a medium having a susceptibility χ absorbs a power:

$$P = \frac{1}{2}\omega\mu_0 \iiint H^\star \chi" H\ dV \tag{18}$$

While comparing with the equation 11:

$$\chi" = -\frac{(g\mu_B)^2 2\mu_0 \Delta n}{\hbar} g(\nu) \tag{19}$$

By introducing the expressions of Δn (solution of the two levels rate equations) and $g(\nu)$ [3], [11] and by supposing that the frequency of the signal is close to the spin resonance ($\nu \approx \nu_{12}$) wa can expressed the imaginary part of the magnetic susceptibility:

$$\chi" = -2\pi\nu_{12}T_2\chi_0 \frac{1}{1+(2\pi T_2)^2(\nu-\nu_{12})^2 + T_1T_2(\gamma H)^2} \tag{20}$$

where χ_0 is the dc susceptibility:

$$\chi_0 = \frac{(g\beta)^2\mu_0}{kT} N \tag{21}$$

χ' et χ" are connected by the Kramer-Krönig relation and finally we get:

$$\chi(\nu) = \chi'(\nu) + j\chi"(\nu)$$

$$= -2\pi\ T_2\ \nu_{12}\chi_0 \left[\frac{2\pi T_2 \Delta\nu \quad + j}{1+(2\pi T_2)^2(\nu-\nu_{12})^2 + T_1T_2(\gamma H)^2} \right] \tag{22}$$

For a very weak signal being propagated in the resonator ($T_1T_2(\gamma H)^2 \ll 1$). The magnetic susceptibility induces losses and a considerable frequency shift of the whispering gallery modes located on both sides of the spin resonance. When the intensity of the signal increases, the saturation of the transition decreases the influence of χ.

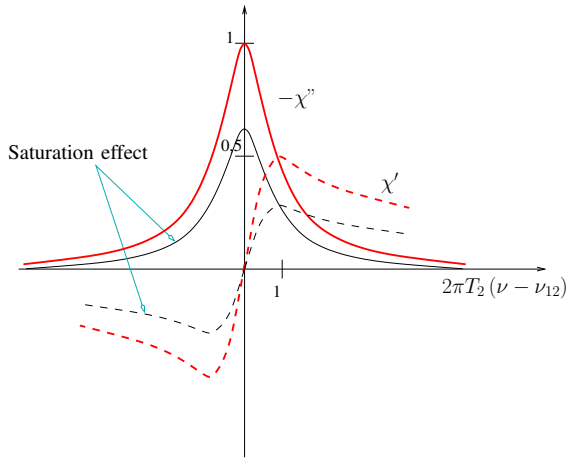

Fig. 9. *Real and imaginary parts of the magnetic susceptibility (arbitrary unities).*

The real part χ' extends very largely around the center frequency. χ' induces a displacement of frequency of the various gallery modes located on both sides of the spin resonance. This property was used to determine the spin-spin relaxation time T_2.

C. The resonator behavior equation

1) Dephasing along a turn: While taking in consideration the presence of the parmagnetic ions, the dephasing (eq.8) becomes:

$$\Phi = \frac{4\pi^2 R_e \nu}{c}\sqrt{\epsilon_z}\left[1 + \frac{\chi'_{eff}}{2} + j\frac{\chi"_{eff}}{2}\right] \tag{23}$$

χ_{eff} is the effective susceptibility of the resonator taking into account the distribution of the magnetic field:

$$\chi_{eff}(\nu) = \frac{\int H^\star(r)\chi(\nu,r)H(r)dV}{\int H^\star H dV} \equiv \eta\chi(\nu) \tag{24}$$

where η is the magnetic filling factor, and $\chi(\nu)$ the susceptibility of the material in the presence of a homogenous magnetic field of intensity equal to the peak value of the field in the real resonator.

By introducing $\Delta\nu_0 = \nu - \nu_0$: the frequency shift between the signal and the resonance of the whispering gallery mode, it comes:

$$\Phi = \frac{4\pi^2 R_e \nu_0}{c}\sqrt{\epsilon_z}\left(1+\frac{\Delta\nu_0}{\nu_0}\right)\left[1 + \frac{\chi'_{eff}}{2} + j\frac{\chi"_{eff}}{2}\right] \tag{25}$$

$$\Phi - 2m\pi = m\pi\left[2\frac{\Delta\nu_0}{\nu_0} + \chi'_{eff} + j\chi"_{eff}\right] \tag{26}$$

2) The internal magnetic field H: To introduce the ions resonance saturation farther, it's necessary to express the magnetic field in the resonator on the way (bias) of the line transmission model. The wave a_+ in any resonator plan is connetcted to the outgoing wave (boils) b_{out} as follow:

$$|b_{out}| = \sqrt{2}jk_2|a_+| \tag{27}$$

The average power circulating in the resonator is equal to:

$$Power = \frac{1}{2}\frac{a_+^2}{Z_C} \tag{28}$$

Where Z_C is the whispering gallery mode impédance.
Moreover, in terms of magnetic field, this power can be expressed according to the Poynting vector:

$$Power = \nabla\bullet\Re\left[\int_{surface}\frac{1}{2}\mathbf{E}_+ \times \mathbf{H}_+ dS\right] \equiv \frac{1}{2}Z_C|H_+|^2 \times S_{eff} \tag{29}$$

where S_{eff} is the effective area which depends on the distribution of the field in the meridian section of the resonator. It corresponds at first approximation to wide of the mode in the plan (ρ,θ). An approximation of this value is given by:

$$S_{eff} \approx h_S\frac{R_e}{\sqrt{m}} \tag{30}$$

Finally:

$$|a_+| = Z_C\sqrt{S_{eff}}|H_+| \tag{31}$$

The total magnetic field results from the establishment of a standing wave in the resonator is then expressed as:

$$H(\theta) = \frac{2|a_+|}{Z_C\sqrt{S_{eff}}}cos(m\theta) \tag{32}$$

To solve the problem analytically, we will use the approximation of the average field. This approximation amounts replacing the local value of the field by its average value. Thus gums the space variations of the magnetic field

$$H^2(\theta) \rightarrow \left\langle \left(\frac{2\left|a_+\right|}{Z_C\sqrt{S_{eff}}} cos(m\theta) \right)^2 \right\rangle = \frac{2\left|a_+\right|^2}{Z_C^2 S_{eff}} \quad (33)$$

3) Coefficient of saturation : In the preceding expressions 15,22, saturation appears in the denominator in the form of $T_1T_2\left(\gamma H\right)^2$. This term defines the amplitude of saturation $|a_{sat}|$ for which the preceding term is equal to the unit. When the amplitude of the wave circulating in the resonator is equal to $|a_{sat}|$, the difference of population Δn is equal to half of the population difference ΔN corresponding to thermodynamic equilibrium:

$$|a_{sat}| = \frac{Z_C\sqrt{S_{eff}}}{\gamma\sqrt{2T_1T_2}} \quad (34)$$

Finally the saturation coefficient X is defined as:

$$X^2 = T_1T_2\left(\gamma H\right)^2 = \frac{\left|a_+\right|^2}{\left|a_{sat}\right|^2} \quad (35)$$

4) Fundamental equation: To complete this model we have now to connect the injected power in the resonator to the power circulating in this one:

$$b_{out} = \sqrt{2}jk_2a_+ = S_{21}a_{in} \quad (36)$$

From the expression of eq.7 and eq26 we can write:

$$2\left|a_+\right|^2\left[\left(\frac{1}{Q_L^{WG}} - \chi"_{eff}\right)^2 + \left(2\frac{\Delta\nu_0}{\nu_0} + \chi'_{eff}\right)^2\right] = \left(\frac{k_1}{m\pi}\right)^2\left|a_{in}\right|^2 \quad (37)$$

the substitution of χ' and χ" expressions, and with $\Delta = 2\pi T_2\left(\nu - \nu_{12}\right)$:

$$2X^2\left[\left(1+\frac{\eta Q_L^{WG}2\pi T_2\nu_{12}\chi_0}{1+\Delta^2+X^2}\right)^2 + \left(2\frac{\Delta\nu_0}{\nu_0}Q_L^{WG} - \frac{\eta Q_L^{WG}2\pi T_2\nu_{12}\chi_0\Delta}{1+\Delta^2+X^2}\right)^2\right] = \left(\frac{k_1Q_L^{WG}}{m\pi}\right)^2\frac{\left|a_{in}\right|^2}{\left|a_{sat}\right|^2} \quad (38)$$

To connect this model to the experimental parameters, the coefficient of saturation X^2 is rewritten as:

$$X^2 \equiv \frac{\left|a_+\right|^2}{\left|a_{sat}\right|^2} \equiv \frac{1}{2k_2^2}\frac{\left|b_{out}\right|^2}{\left|a_{sat}\right|^2} \equiv \frac{Q_0^{WG}}{4m\pi\beta_2}\frac{Z_0}{Z_C}\frac{P_{out}}{P_{sat}} \quad (39)$$

where $Z_0 = 50\Omega$ is the microwave characteristic impedance. It is noted that X^2 is proportional to the emmited power.

To simplify the last equation we define the following parameters:

Y^2 who is proportional to the injected power:

$$Y^2 \equiv \frac{2\beta_1}{\left(1+\beta_1+\beta_2\right)^2}\frac{Q_0^{WG}}{m\pi}\frac{Z_0}{Z_C}\frac{\left|P_{in}\right|}{\left|P_{sat}\right|} \quad (40)$$

C called Cooperativity which is a parameter indicating the degree of non-linearity of the system:

$$C \equiv \eta Q_L^{WG}\pi T_2\nu_{12}\chi_0 \equiv \eta Q_L^{WG}Q^{EPR}\chi_0 \quad (41)$$

where Q^{EPR} is the quality factor of the paramagnetic resonance line shape: $Q^{EPR} = \pi T_2\nu_{12}$.

Finally ξ is the ratio between the instantaneous frequency deviation $\nu_0 - \nu$ and the half-width of the mode for the charged resonator.

$$\xi = 2\frac{\Delta\nu_0}{\nu_0}Q_L^{WG} \quad (42)$$

Finally the resonator behavior equation is summarized with:

$$2X^2\left[\left(1+\frac{2C}{1+\Delta^2+X^2}\right)^2 + \left(\xi - \frac{2C\Delta}{1+\Delta^2+X^2}\right)^2\right] = Y^2 \quad (43)$$

In a simple case: the mode and the signal are both centered on paramagnetic resonance: $\Delta = \varphi = 0$, the equation is thus reduced to:

$$2X^2\left(1+\frac{2C}{1+X^2}\right)^2 = Y^2 \quad (44)$$

For a linear resonator, the ratio between the injected and emmited power is still constant whatever the level of the injected signal is. The presence of the paramagnetic ions induces the appearance of extremum in the representation of P_{out} according to P_{in}. This means that the condition to obtain it, is:

$$\frac{d\left(Y^2\right)}{d\left(X^2\right)} = 0 \quad (45)$$

After a simple calculation, the equality is realized if:

$$\left(X^2+1-C\right)^2 = C(C-4) \quad (46)$$

The bistability thus will appear if $C > 4$. Then it is possible to calculate the values of X^2 and Y^2 corresponding to the extrema.

The relation can be reexpress according to the powers:

$$P_{in} = \Lambda P_{out}\left(\left(1+\frac{2C}{1+\Delta^2+\frac{Q_0^{WG}}{4m\pi\beta_2}\frac{Z_0}{Z_C}\frac{P_{out}}{P_{sat}}}\right)^2 + \left(\xi - \frac{2C\Delta}{1+\Delta^2+\frac{Q_0^{WG}}{4m\pi\beta_2}\frac{Z_0}{Z_C}\frac{P_{out}}{P_{sat}}}\right)^2\right) \quad (47)$$

with $\Lambda = \frac{\left(1+\beta_1+\beta_2\right)^2}{4\beta_1\beta_2} = \left(\frac{1}{S_{21}}\right)^2$

This equation shows the role which the couplings can have. The factor Λ is identified as the reverse of the square of the transmission coefficient.

D. Magnetic susceptibility measurement

In a pure sapphire resonator (i.e. in impurity free region), the frequency of the WG mode depends only on the geometry and on permittivity of the material. The Fe^{3+} paramagnetic impurities induce a magnetic susceptibility in the resonator which yields to shift the resonant frequencies of the different WGH modes around the ESR resonance at 12.04 GHz.

If a strong signal at 12.04 GHz is applied to the resonator, the power absorbed by the magnetic resonance is no longer proportional to the incident power, but rather saturates. This led to a frequency shift of the surrounding WG modes back to the one they should have had in the abscence of impurities. This is explained by the fact that the magnetic susceptibility, which is proportional to the difference in population of the two lower levels, tends to zero.

The real part of the ac magnetic susceptibility is given by :

$$\chi' = \frac{4\pi^2 T_2^2 \chi_0 \nu_0 \Delta\nu}{1 + 4\pi^2 T_2^2 \Delta\nu^2} \tag{48}$$

where T_2 is the spin-spin decoherence time, χ_0 the dc-susceptibility, and $\Delta\nu$ the detuning parameter of the analysed WG mode with respect to the ESR-line (ν_0) and assuming that the energy is totally confined inside the sapphire (magnetic filling factor $\eta \sim 1$).

The measurement set-up is then represented in figure 11.

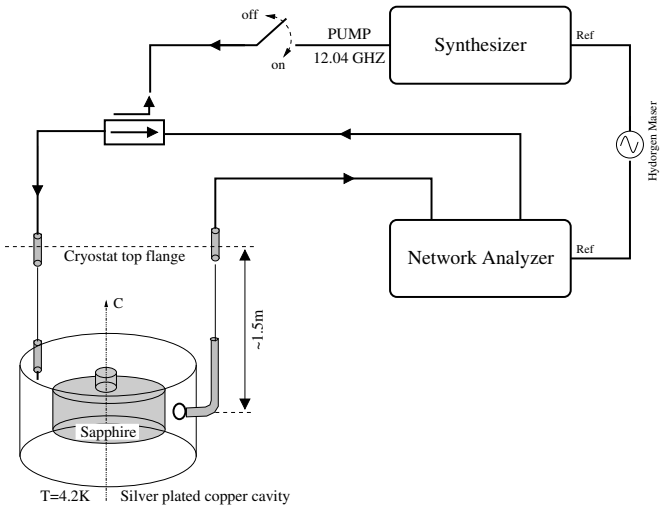

Fig. 10. Set-up for electron paramagnetic resonance experiment.

A pump signal corresponding to the $WGH_{17,0,0}$ mode is sent to the resonator with the help of an external microwave synthesizer. The power -of about 3dBm- is high enough to saturate the transition. The detuned frequencies of each mode around $WGH_{17,0,0}$ are recorded via a network analyser. The real part of the magnetic susceptibility can be then evaluated and subsequently plotted as a function of the measured detuned parameter, as shown in figure 11.

An adapted fit to this curve related on eq. (48) give the dc susceptibility $\chi_0 \approx 10^{-9} \pm 0.1 \times 10^{-9}$ and the spin-spin relaxation time $T_2 \approx 2.2 \times 10^{-9}\text{s} \pm 0.8 \times 10^{-9}\text{s}$.

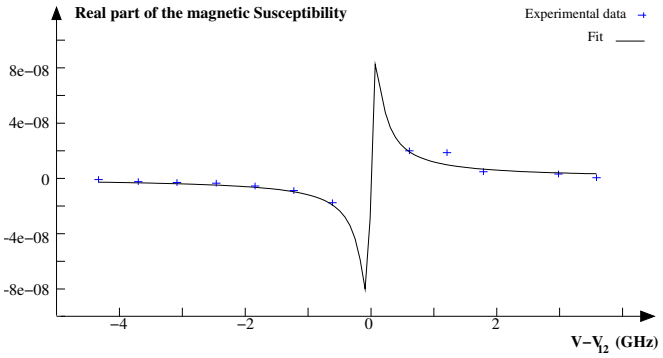

Fig. 11. $\chi' = -2\frac{\Delta\nu}{\nu}$

These values are of about one order of magnitude from other measurements [2]. As a matter of fact, the width of the ESR-line is known to be approximately equal to 27 MHz [3]. The equivalent Q-factor Q_{ESR} is then ≈ 450, therefore :

$$Q_{ESR} = \pi\nu_0 T_2 \tag{49}$$

Eq. (49) give $T_2 \approx 10^{-8}$, which is consistent with other measurements. A possible explanation of this discrepancy is the inaccuracy of the data fit due to the lack of data points near the sharp variation region of χ'.

A more physical one is also given there.

At thermal equilibrium, dc-susceptibility χ_0 can be given by :

$$\chi_0 = \frac{(g\beta)^2 \mu_0}{4k_B T} N \tag{50}$$

with g the Landé factor $\sim$ 2, β Bohr's magneton $= 9.27 \times 10^{-24}\text{Am}^2$, k_B the Boltzmann constant, and N the iron ions concentration. One can then evaluate the iron ions concentration to be $5.3 \times 10^{20}\text{ions m}^{-3}$. We have already pointed out that such a small concentration ($\approx$ 12 ppb) is enough to obtain a maser operation. This result is also consistent with our previous estimation based on the measured maser power [4]. However this value is far less than the Fe^{3+} ions concentrations obtained by spectroscopic methods in HEMEX sapphire samples [7] of about 2 ppm. This inconsistency may be explained by assuming the 12.04 GHz absorbtion line shape is inhomogeneously broadened [8] which led to a spin-spin relaxation time $T_2^\star << T_2$. Most of the spins have different precessional frequencies than in a homogeneous broadening situation. Their resonant structure is also known as *spin-packet.*

IV. Spin lattice relaxation times

It has been shown (in the early 60s) [5], [6] that the determination of the spin-lattice relaxation time T_1 is more adapted using a time domain technique. The principle of this experiment was inspired from [6]. and is schematized in figure 12.

We build an oscillator loop around the cryogenic sapphire resonator. A cavity filter placed in this loop permits to get oscillation on the $WGH_{18,0,0}$ mode at 12.654 GHz. This

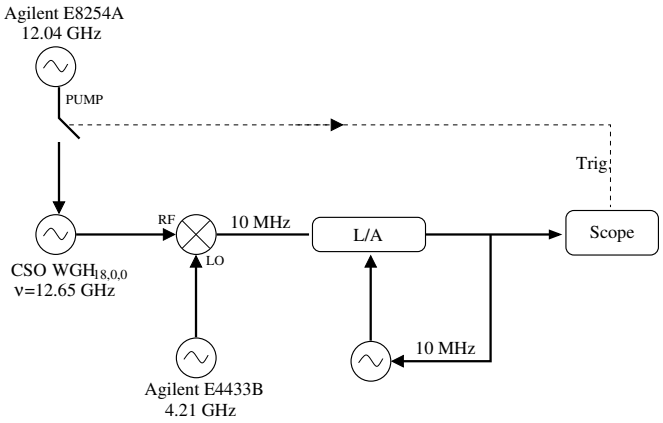

Fig. 12. Principle of spin-lattice relaxation time measurement.

mode was chosen because its frequency shift observed in the previous section is large: 120Hz. A microwave coupler is used to inject (in the loop at the resonator input) the signal coming from a synthesizer tuned to the ESR at 12.04 GHz. A power of -6dBm is sufficient to saturate the ESR. The oscillator output is sent to a specially designed system to analyze the fast change in the oscillator frequency when the pump is switched. The frequency of the analysed signal is firstly down-converted to low frequencies (10 MHz) by mixing it with an external microwave synthesizer. A 10 MHz VCO phase locked on this signal. The low frequency error signal is then an image of the VCO frequency and follows the frequency of the CSO. When the pump is switched on, the frequency change is recorded on an oscilloscope trigged to the microwave synthesizer pump via a quadratic detector.

We volontary increased the resonator coupling in order to get a loaded Q-factor of $30 \cdot 10^6$. Under these conditions, the intrinsic relaxation time of the resonator is 1 ms which is about ten times lower than the expected value of T_1. Figure 13

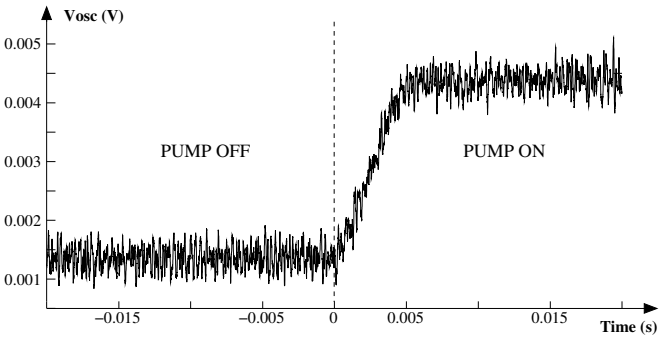

Fig. 13. Oscilloscope trak example.

shows an example of the observed signal during a 12.04 GHz pump-on/off cycle. As the voltage is directly proportionnal to the oscillator frequency, T_1 is determined by the time constant of this exponential function, that is $T_1 = 10$ ms.

A. Theory vs experiment

By injecting all the preceeding measured parameters into the resonator behavior state equation **??**, one can now verify that the model fits in a good agreement with our observations, as represented on the figure 14

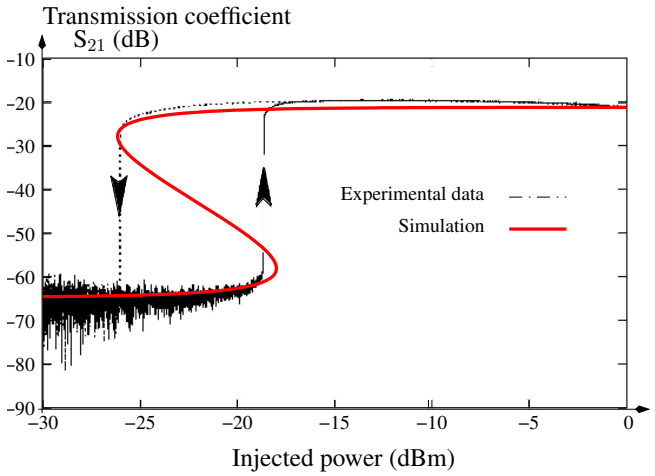

Fig. 14. Theory and experimental observations confrontation.

V. Conclusion

In this paper we have presented the new pretendant to the ultrastable secondary frequency standards, the whispering gallery mode maser oscillator. In terms of frequency instability we could compare the maser to a state-of-the-art cryogenic sapphire resonator oscillator while implementing a necessary microwave synthesis chain locked to the CSRO. The frequency instability is short-term limited by the readout system at 10^{-14} until 30 seconds integration times, and mid-term degraded by a random walk process. We have also presented the resonator bistability behavior and review some theoretical aspects to analyse this phenomena which ultimately conduct to a fundamental state equation. By applying several measurement processes (magnetic susceptibility, relaxation times) to put numbers into that equation, we have finally verified that our models described nicely the resonator behavior. It is worth to note that it constitutes the first step to an overall WGMO theory which will include the fields and the completed coupling system.

The Whispering gallery mode maser oscillator has got great potentialitites. It is already 10 000 times more powerful than a hydrogen maser, but we suspect that it could delivers even more microwave power. All the oscillator is placed at cryogenic temperature and within the resonator itself. As a maser, it is mainly limited by the thermal noise thus may have interesting properties about phase noise compared to the 'traditional' CSRO :

$$S_\phi(f) = \frac{k_B T}{P} \tag{51}$$

For $P = 10$ nW at liquid helium temperature, this led to S_ϕ= $-145\text{dbrad}^2/\text{Hz}$ at 1 Hz. Concerning then the frequency

instability, the Allan deviation could be rewritten as :

$$\sigma_y(\tau) = \frac{1}{Q}\sqrt{\frac{k_B T}{2P\tau}} \tag{52}$$

For a Q-factor as low as 5×10^8, the theoretical behavior of Allan deviation is $\sigma_y(\tau) = 1.5 \times 10^{-16}\tau^{-1/2}$.

ACKNOWLEDGMENT

Our works are funded by the Agence Nationale de la Recherche, The french space agency CNES. Special thanks to the FAST program funded by Egide for French-Australian travels supports.

P.-Y. Bourgeois wishes kindly to say "un grand merci" to the IEEE-IFCS/EFTF 2007 Joint meeting technical committee for invited author and acknowledge Giorgio Santarelli for very useful discussions.

REFERENCES

[1] P.-Y. Bourgeois, N. Bazin, Y. Kersalé, V. Giordano, M.E. Tobar and M. Oxborrow, *Maser Oscillation in a Whispering-Gallery-Mode Microwave Resonator*, App. Phys. Lett., vol. 87,224104-1-3, 2005.

[2] A.G. Mann, A.J. Giles, D.G. Blair and M.J. Buckingham, *Ultra-stable cryogenic sapphire dielectric microwave resonators: mode frequency-temperature compensation by residual paramagnetic impurities*, J. Phys. D. Appl. Phys., vol 25, 1991.

[3] H.F. Symmons and G.S. Bogle, *On the exactness of the Spin-Hamiltonian description of Fe3+ in sapphire*, Proc. Phys. Soc., vol 79, 1962.

[4] P.-Y. Bourgeois, M. Oxborrow, N. Bazin, Y. Kersalé, M. E. Tobar and V. Giordano, Proc. 19th European Frequency and Time Forum, Besançon, France, 2005.

[5] M. W. P. Strandberg, *Spin-lattice relaxation*, Phys. Rev., vol 110, n 1, 1958.

[6] C. F. Davis, Jr., M. W. P. Strandberg and R. L. Kyhl, *Direct measurement of electron spin-lattice relaxation times*, Phys. Rev., vol 111, n 5, 1958.

[7] *Trace element studies in HEM sapphire*, LCS six-month progress report LIGO-M0303366-00-M organization: Department of Physics, Southern University and AM College, 2003

[8] A. M. Portis, *Electronic structure of F-centers: saturation of the electron spin resonance*, Phys. Rev., vol 91, n 5, 1953.

[9] L. A. Lugiato, Progress in Optics, (Edited by E. Wolf, Elsevier, 1984).

[10] P.-Y. Bourgeois and V. Giordano, *Simple Model for the Mode-Splitting Effect in Whispering-Gallery-Mode Resonators*, IEEE Trans. Mic. Theo. Tech., vol 53,n 10 ,2005.

[11] A. E. Siegman, *Microwave Solid-state Masers*, McGraw Hill, 1964.